



HAL
open science

Hydroboration of Alkenes Catalysed by a Nickel N-Heterocyclic Carbene Complex: Reaction and Mechanistic Aspects

Franck Ulm, Yann Cornaton, Jean-Pierre Djukic, Michael Chetcuti, Vincent Ritleng

► **To cite this version:**

Franck Ulm, Yann Cornaton, Jean-Pierre Djukic, Michael Chetcuti, Vincent Ritleng. Hydroboration of Alkenes Catalysed by a Nickel N-Heterocyclic Carbene Complex: Reaction and Mechanistic Aspects. *Chemistry - A European Journal*, 2020, 26 (41), pp.8916-8925. 10.1002/chem.202000289 . hal-02921998

HAL Id: hal-02921998

<https://hal.science/hal-02921998>

Submitted on 4 Jan 2021

HAL is a multi-disciplinary open access archive for the deposit and dissemination of scientific research documents, whether they are published or not. The documents may come from teaching and research institutions in France or abroad, or from public or private research centers.

L'archive ouverte pluridisciplinaire **HAL**, est destinée au dépôt et à la diffusion de documents scientifiques de niveau recherche, publiés ou non, émanant des établissements d'enseignement et de recherche français ou étrangers, des laboratoires publics ou privés.

Hydroboration of alkenes catalysed by a nickel N-heterocyclic carbene complex: reaction and mechanistic aspects

Franck Ulm,^[a] Yann Cornaton,^[b] Jean-Pierre Djukic,^[b] Michael J. Chetcuti,^{*[a]} and Vincent Ritleng^{*[a],[c]}

Abstract: The pentamethylcyclopentadienyl N-heterocyclic carbene nickel complex $[\text{Ni}(\eta^5\text{-C}_5\text{Me}_5)\text{Cl}(\text{IMes})]$ (IMes = 1,3-dimesitylimidazol-2-ylidene) efficiently catalyses the anti-Markovnikov hydroboration of alkenes with catecholborane in the presence of a catalytic amount of potassium *tert*-butoxide, and joins the very exclusive club of nickel catalysts for this important transformation. Interestingly, the regioselectivity can be reversed in some cases by using pinacolborane instead of catecholborane. Mechanistic investigations involving control experiments, ^1H and ^{11}B NMR spectroscopy, cyclic voltammetry, piezometric measurements and DFT calculations suggest an initial reduction of the Ni(II) precursor to a Ni(I) active species with the concomitant release of H_2 . The crucial role of the alkoxy-catecholato-borohydride species resulting from the reaction of potassium *tert*-butoxide with catecholborane in the formation of an intermediate nickel-hydride species that would then be reduced a Ni(I) active species, is highlighted.

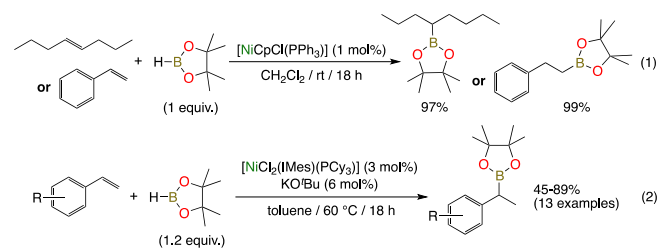
Introduction

Boronic acid and ester derivatives are important starting materials in molecular synthesis and are well-known partners for classical transformations, such as the Petasis reaction,¹ Chan–Lam coupling,² conjugate addition reactions,³ and, most impressively, Suzuki–Miyaura cross-couplings,⁴ but their traditional production methodology involves a metal–halogen exchange with an organoalkali reagent and trialkylborates,⁵ which is far from being satisfying from an environmental perspective. Subsequently, new methods were developed through the direct borylation of aryl halides, mostly catalysed by Pd.⁶ More recent advances have allowed the hydroboration of alkenes,⁷ a reaction which is of great interest since the substrates are readily available and it creates new C–B bonds by the most straightforward and atom-thrifty synthetic route.

The main drawback of this methodology is that it is principally based on noble metals, such as rhodium and iridium.⁷ The decrease in non-renewable natural resources has indeed become a global concern for the future, and precious transition metals, are, just like to fossil fuels, limited and thus strategic resources. This can be monitored by the tremendous increase of their prices over the last decade. New directions for homogeneous catalysis should thus not only address energy issues by developing highly reactive catalysts, but should also favour the use of earth-abundant materials as catalysts.

In this context, complexes based on first-row transition metals,⁸ most notably copper,⁹ cobalt,¹⁰ iron,¹¹ and manganese¹² have recently emerged as alternative catalysts for this process. In contrast, although it has shown promise for the hydroboration of alkynes,¹³ the 1,4-hydroboration of 1,3-dienes,¹⁴ or more recently for formal hydroborations making use of a diboron reagent with a proton source,¹⁵ there are to our knowledge only three reports of the nickel-catalysed hydroboration of alkenes.¹⁶ The first one involved an activated nickel powder that showed relatively low activity and selectivity.^{16a} In the two other examples, well-defined nickel(II) pre-catalysts were used, which showed excellent activity and selectivity. Hence, in 1996, Srebnik *et al.* reported that the half-sandwich triphenylphosphine nickel complex, $[\text{Ni}(\text{Cp})\text{Cl}(\text{PPh}_3)]$ (Cp = $\eta^5\text{-C}_5\text{H}_5$), catalyses the selective hydroboration of *trans*-4-octene and styrene with HBPIn to give 4-pinacolboryloctane and 1-phenyl-2-pinacolborylethane in high yields (Scheme 1, eq. 1).^{16b} In contrast, Schomaker *et al.* recently reported that the heteroleptic NHC-phosphine nickel complex, $[\text{NiCl}_2(\text{IMes})(\text{PCy}_3)]$ (IMes = 1,3-dimesitylimidazol-2-ylidene), catalyses the Markovnikov-selective hydroboration of styrenes with good efficiency in the presence of KO*t*-Bu (Scheme 1, eq. 2).^{16c} Remarkably, no dehydroborylation product was observed in both cases, but the reaction scopes were rather limited, and no mechanistic study was carried out.

- [a] F. Ulm, Prof. M. J. Chetcuti, Prof. V. Ritleng
 Université de Strasbourg
 Ecole européenne de Chimie, Polymères et Matériaux
 CNRS, LIMA UMR 7042
 F-67000 Strasbourg, France
 E-mail: michael.chetcuti@unistra.fr, vritleng@unistra.fr
- [b] Dr. Y. Cornaton, Dr. J.-P. Djukic
 Université de Strasbourg
 CNRS, Institut de Chimie de Strasbourg UMR 7177
 F-67000 Strasbourg, France
- [c] Prof. V. Ritleng
 Institut Universitaire de France
 1 rue Descartes, F-75000 Paris, France



Scheme 1. Previously reported nickel-catalysed hydroboration of alkenes.^{16b,c}

In parallel, efforts from our group and others towards the diversification of pseudo-trigonal $[\text{Ni}(\eta^5\text{-C}_5\text{R}_5)\text{L}(\text{NHC})]^{(+)}$ species and the study of their catalytic activity in a large array of reactions, have allowed their establishment as a highly versatile platform for important organic transformations.¹⁷ Most notably, interesting activities have been obtained for the hydrosilylation of carbonyl¹⁸ and imine¹⁹ derivatives. Thus, the half-sandwich nickel complex, $[\text{Ni}(\text{Cp})\text{Cl}(\text{IMes})]$ (**1a**), was shown to efficiently catalyse the hydrosilylation of a vast array of aldehydes, ketones, aldimines and ketimines (over 60 examples!) under mild conditions in the presence of a catalytic amount of sodium borohydride.^{18a,19} This precedent, together with (i) the scarcity of nickel-catalysed alkene hydroborations,¹⁶ (ii) the electronic and structural proximity of $[\text{Ni}(\text{Cp})\text{Cl}(\text{PPh}_3)]$ and **1a**, (iii) the renewed interest in the fascinating chemistry of nickel,²⁰ and (iv) the necessity to gain a better understanding of its reaction paths in order to be able to tame its reactivity, prompted us to enter this challenging field with a series of $[\text{Ni}(\text{Cp}^+)\text{L}(\text{NHC})]^{(+)}$ complexes ($\text{Cp}^+ = \text{Cp}$, $\text{Cp}^* (\eta^5\text{-C}_5\text{Me}_5)$; $\text{L} = \text{Cl}$, NCMe , $\text{NHC} = \text{IMes}$, IPr (1,3-bis(2,6-diisopropylphenyl)imidazol-2-ylidene), ICy (1,3-dicyclohexylimidazol-2-ylidene) and to try to unravel the mechanism at play.

Herein, we show that the Cp^* complex, $[\text{Ni}(\text{Cp}^*)\text{Cl}(\text{IMes})]$ (**2a**), efficiently catalyses the *anti*-Markovnikov hydroboration of alkenes with HBCat (catecholborane) in the presence of a catalytic amount of $\text{KO}t\text{-Bu}$. Notably, the selectivity can be reversed for some styrene derivatives by using HBPIn (pinacolborane) instead of HBCat. A combination of experiments gives some insight to the mechanism. The latter is proposed to go through a $\text{Ni}(\text{I})/\text{Ni}(\text{III})$ cycle after initial reduction of the nickel(II) precursor by a *tert*-butoxo-catecholato-borohydride species.

Results and Discussion

Initial studies focussed on the hydroboration of styrene with HBPIn in CH_2Cl_2 at room temperature, conditions under which the complex $[\text{Ni}(\text{Cp})\text{Cl}(\text{PPh}_3)]$ (1 mol%) had been reported to quantitatively convert styrene to 1-phenyl-2-pinacolborylethane in 18 h (Scheme 1, eq. 1).^{16b} Disappointingly however, absolutely no conversion was observed under these conditions with the closely related complexes, **1a** and $[\text{Ni}(\text{Cp})\text{Cl}(\text{IPr})]$ (**1b**). Intrigued by this negative result, we reinvestigated the reaction with $[\text{Ni}(\text{Cp})\text{Cl}(\text{PPh}_3)]$ and were unable to reproduce Srebnik's result.

We thus decided to investigate the reaction in toluene at 60 °C in the presence of 3 mol% of nickel precatalyst and 6 mol% of $\text{KO}t\text{-Bu}$.^{16c} Under these conditions, **1a** proved again to be unreactive (Fig. 1). A first hit was observed with **1b** with 30% conversion after 18 h and 64% Markovnikov selectivity, but the Cp derivatives proved to be globally poorly reactive, as was also illustrated by the very poor conversion observed with $[\text{Ni}(\text{Cp})\text{Cl}(\text{ICy})]$ (**1c**). A net gain of activity was observed with the electron-rich Cp^* derivatives, notably with **2a** that allowed 75% conversion with a 40:60 *anti*-Markovnikov/Markovnikov (AM/M) ratio. The IPr derivative **2b** proved a little less active in this case,

with 59% conversion after 18 h, and showed no selectivity. Complex **2a** was thus chosen for the optimization study of the reaction conditions (Table 1).

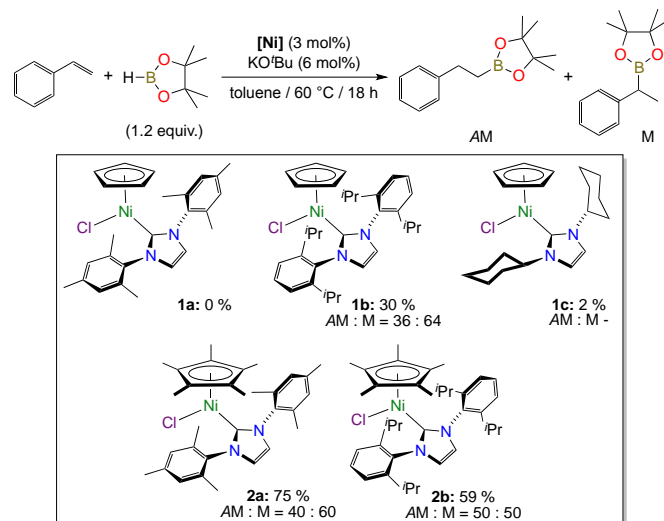


Figure 1. Pre-catalysts' screening for the hydroboration of styrene with HBPIn.

The promising result obtained in 15 h at 60 °C (entry 1) prompted us to decrease the temperature to 25 °C. This resulted in a much better selectivity with a AM/M ratio of 26:74, but the conversion decreased to 62 % (entry 2). Running the reaction for 24 h at 25 °C allowed us to almost reach the conversion observed after 15 h at 60 °C (entry 3). Carrying out the same

Table 1. Hydroboration of styrene with HBPIn or HBCat catalysed by **2a**

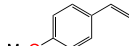
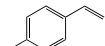
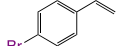
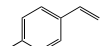
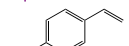
Entry	Borane (equiv.)	Temp. (°C)	Time (h)	Reaction	
				Conv. (%) ^[b]	AM/M (%) ^[b]
$\text{Styrene} + \text{H-B(OR)}_2 \xrightarrow[\text{toluene / 25-60 }^\circ\text{C / 15-24 h}]{\text{2a (3 mol\%)} \text{ KO}t\text{-Bu (6 mol\%)}} \text{AM} + \text{M}$					
1	HBPIn (1.2)	60	15	74	40:60
2	HBPIn (1.2)	25	15	62	26:74
3	HBPIn (1.2)	25	24	70	25:75
4	HBPIn (1.2)	60	24	100	39:61
5	HBPIn (2.5)	60	15	100	20:80
6	HBCat (1.2)	60	15	73	50:50
7	HBCat (1.8)	60	15	83	67:33
8	HBCat (2.5)	60	15	100	85:15
9	HBCat (2.5)	25	15	33	100:0
10 ^[c]	HBCat (2.5)	60	15	100	85:15

[a] Reaction conditions: styrene (1.04 mmol), **2a** (3 mol%), KO^tBu (6 mol%) in toluene (2 mL). [b] Conversions and AM/M ratio determined by ¹H NMR spectroscopy with 1,3,5-trimethoxybenzene as an internal standard; average values of at least two runs. [c] Reaction run with NaO^tBu or LiO^tBu instead of KO^tBu.

catalysis at 60 °C led to full conversion, but still with a low selectivity (entry 4). Finally, increasing the number of equivalents of HBPIn to 2.5 allowed us to observe full conversion as well, but surprisingly with an even better AM/M ratio of 20:80 than at room temperature (entry 5). However, the impossibility, at least in our hands, to cleanly separate the isomers by column chromatography led us to explore the reaction with HBCat. A similar result to HBPIn (1.2 equiv.) at 60 °C (entry 1) was observed with HBCat, with 73 % conversion and a 50:50 AM/M ratio after 15 h reaction (entry 6). Increasing the number of equivalents to 1.8 and 2.5 allowed the conversion to reach 83 and 100%, respectively, but with a reverse regioselectivity (entries 7 and 8), as was recently observed with an aryloxy-tethered NHC-Fe(II) catalyst.²¹ Indeed, in this case, the linear isomer was the major product, and a 85:15 AM/M ratio was obtained when 2.5 equiv. of HBCat were used (entry 8). In light of the increased selectivity observed at room temperature with 1.2 equiv. of borane (entries 2 and 3), we then decided to check if a similar tendency could be observed in the presence of 2.5 equiv. of borane. The *anti*-Markovnikov isomer was the sole product formed under these conditions, but the conversion was only 33 % after 15 h (entry 9). Finally, the replacement of potassium *tert*-butoxide by sodium or lithium *tert*-butoxide had no consequence on the reaction (entry 10).

With these optimized conditions in hand (2.5 equiv. borane,

Table 2. Hydroboration of alkenes with HBCat catalysed by **2a**^[a]

Entry	Substrate	Conv. (%) ^[b]	AM/M (%) ^[b]	Yield (%) ^[c]
1		100	85:15	80
2 ^[d]		100	85:15	72
3		100	100:0	85
4		100	89:11	86
5		100	100:0	52
6		93	85:15	40
7		100	60:40	59
8		100	100/0	79
9		67	80/20	38
10		100	100/0	60

[a] Reaction conditions: alkene (1.0 mmol), HBCat (2.5 mmol), **2a** (3

mol%), KO^tBu (6 mol%) in toluene (2 mL) at 60 °C for 15 h. [b] Conversions and AM/M ratio determined by ¹H NMR spectroscopy with 1,3,5-trimethoxybenzene as an internal standard; average values of at least two runs. [c] Isolated yield of the AM isomer. [d] [NiCp*(NCMe)(IMes)]PF₆ (**3a**) was used as precatalyst instead of **2a**.

toluene, 60 °C, 15 h), we then examined the scope of the hydroboration of alkenes catalysed by **2a** with HBCat (Table 2). Electron-neutral and electron-rich styrenes were all fully converted with high linear selectivity (entries 1-5). In the cases of 4-methoxystyrene and 2-methylstyrene, the linear isomer was actually the sole product (entries 3 and 5). Electron-poor styrenes were hydroborated with conversions ranging from moderate in the case 4-trifluoromethylstyrene (entry 9) to full with 2-bromo- and 4-fluoro-styrenes (entries 7 and 8). With the exception of 2-bromostyrene, which was converted with a poor selectivity, the other substrates all gave good to excellent linear selectivity. In all cases where the branched isomer was formed as a minor product, it decomposed on the silica column,²² allowing the isolation of the pure AM isomer in yields ranging from 38 % in the case of 4-trifluoromethylstyrene (entry 9) to 86 % for 4-methylstyrene (entry 4). The reaction is not limited to styrenes, and vinylcyclohexane was fully converted to the linear isomer, allowing its isolation with 60 % yield (entry 10). *Cis*-stilbene was also hydroborated with good efficiency (80 %), but the resulting product decomposed on the column (Fig. 2). In addition, a number of substrates performed either poorly or non-selectively. Thus, *trans*-stilbene and 1-phenylcyclohexene gave no conversion at all, and 1-methylstyrene, 4-cyanostyrene, cinnamyl chloride and 1-heptene²³ gave complicated mixtures despite good to excellent conversions (Fig. 2).

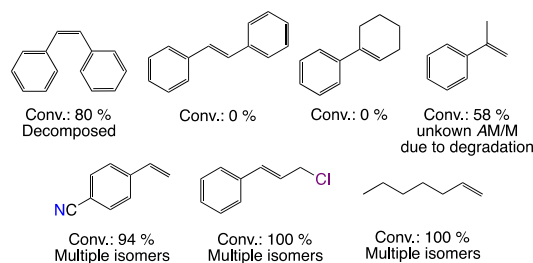


Figure 2. Substrates that performed either poorly or non-selectively with HBCat or that gave a product that decomposed.

As catalysts that can enable different regioselectivities are invaluable for the construction of a diverse set of value-added compounds,⁸ we next also briefly investigated the reaction scope with HBPIn to check if the observed reversal of selectivity with styrene was general (Table 3). Electron-rich and electron-poor styrenes such as 4-methoxystyrene, 2-bromostyrene and 4-trifluoromethylstyrene were also converted to the branched isomer with good to high regioselectivities (entries 2-4). Surprisingly however, 2- and 4-methylstyrene gave the linear isomer quasi-exclusively (entry 5 and 6). Although substrate dependent regioselectivity is observed every now and then,⁹⁻¹² and had, in particular, been noted with the closely related [Ni(Cp)Cl(PPh₃)] for styrene and 4-octene (Scheme 1),^{16b} it is to

our knowledge rarely observed within a series of simple styrene derivatives. We therefore did not pursue our substrate scope investigation with HBPIn any further.

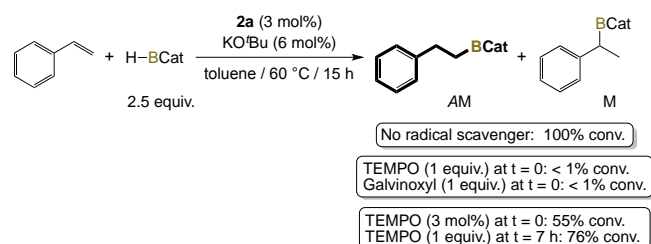
Table 3. Hydroboration of styrenes with HBPIn catalysed by **2a**^[a]

Entry	Substrate	Conv. (%) ^[b]	AM/M (%) ^[b]	Yield (%)
1		100	20:80	-
2		100	26:74	51 ^[c]
3		100	- ^[d]	94
4		100	13:87	95 ^[c]
5		100	99:1	22 ^[e]
6		100	99:1	36 ^[e]

[a] Reaction conditions: alkene (1.0 mmol), HBPIn (2.5 mmol), **2a** (3 mol%), KO^tBu (6 mol%) in toluene (2 mL) at 60 °C for 15 h. [b] Conversions and AM/M ratio determined by ¹H NMR spectroscopy with 1,3,5-trimethoxybenzene as an internal standard; average values of at least two runs. [c] Isolated yield of the AM/M mixture. [d] The AM:M ratio was difficult to evaluate due to the possible presence of debromoborylation products.²⁴ [e] The low isolated yields are due to massive decomposition during the chromatographic purification.

To gain insight to the mechanism, we first checked whether the hydroboration process was the result of a true homogeneous catalysis by conducting the hydroboration of styrene with HBCat in the presence of 190 equivalents of Hg relative to **2a**. No inhibition was observed, nor a change of selectivity, and thus a process catalysed by nickel particles is unlikely.²⁵

Owing to the propensity of nickel to easily access multiple oxidation states,²⁰ we then checked whether the reaction involves a radical by performing control experiments in the presence of radical scavengers. The addition of 1 equiv. of TEMPO or galvinoxyl (relative to styrene) at *t*₀ completely inhibited the reaction (Scheme 2). Furthermore, the addition of 3 mol% TEMPO limited the conversion to 55% after 15h reaction, and the addition of 1 equiv. TEMPO after 7 h reaction to 76% (vs. 100% without radical scavenger). This suggested the presence of radicals not only during the activation phase but during the catalytic cycle itself.



Scheme 2. Effect of radical inhibitors.

This point being established, we then recorded a cyclic voltammogram of the pre-catalyst (1 mM) in CH₃CN (0.1 M NBu₄PF₆). As the latter tended to generate a deposit at the surface of the carbon electrode that altered the reproducibility of the measurements, the electrochemical characterization was carried out with the cationic derivative, [Ni(Cp*)(NCMe)(IMes)]PF₆ (**3a**), of **2a** that shows a similar catalytic activity (Table 2, entry 2). At a scan rate of 200 mV·s⁻¹, a quasi-reversible oxidation process can be observed at E_{1/2ox} = 0.16 V vs. Fc/Fc⁺ (ΔE_p = 154 mV), and a quasi-reversible reduction peak is seen at E_{1/2red} = -1.75 V (ΔE_p = 190 mV) (Fig. 3). By analogy with the electrochemical data reported by Crabtree for the Cp derivative **1a** (E_{1/2ox} = 0.03 V and E_{1/2red} = -1.51 V vs. Fc/Fc⁺, ν = 100 mV·s⁻¹),²⁶ these values most likely correspond to Ni(II)/Ni(III) oxidation and Ni(II)/Ni(I) reduction processes, while the irreversible oxidation and reduction peaks observed at -0.25 V and -1.48 V (vs. Fc/Fc⁺) potential would correspond to ligand-centred redox processes. Nevertheless, the Cp* ligand has been described 'to act as an electron density buffer',²⁷ which might mean that neither of these redox processes are purely metal centred, and could explain the counter-intuitive observation of a higher Ni(II)/Ni(III) oxidation potential for **3a** with respect to **1a**.

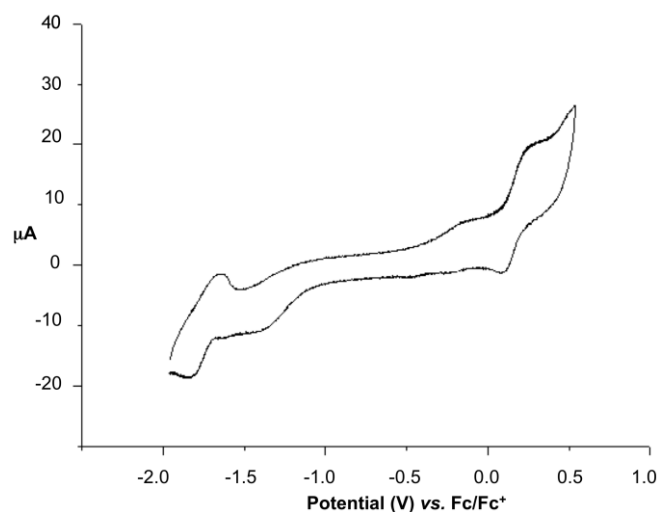


Figure 3. Cyclic voltammogram of **3a**: 1 mM **3a** in a 0.1 M NBu₄PF₆ solution in CH₃CN with a glassy C working electrode, a Pt wire counter electrode, and a Ag/AgCl, KCl 3 M reference electrode. Referenced to a 2mM Fc/Fc⁺ external standard: E_{1/2} = 0.48 V vs. Ag/AgCl, KCl 3 M. Scan rate = 200 mV·s⁻¹.

In parallel, stoichiometric studies were conducted to try to identify reaction intermediates. Thus, we monitored the reaction of **2a** with 1 equiv. of HBCat and 1 equiv. of KO^tBu by ¹H NMR in C₆D₆ from 253 to 298 K. At 293 K, signals belonging to a Cp*-Ni(IMes) species were unambiguously identified (Fig. 4). Though a little broad, these signals are found at the same chemical shifts as those of **2a**, suggesting that most of the starting

complex is unreacted under these conditions. Nevertheless, a singlet observed at 4.47 ppm is assigned to molecular H₂. Furthermore, another singlet, observed at -22.9 ppm and

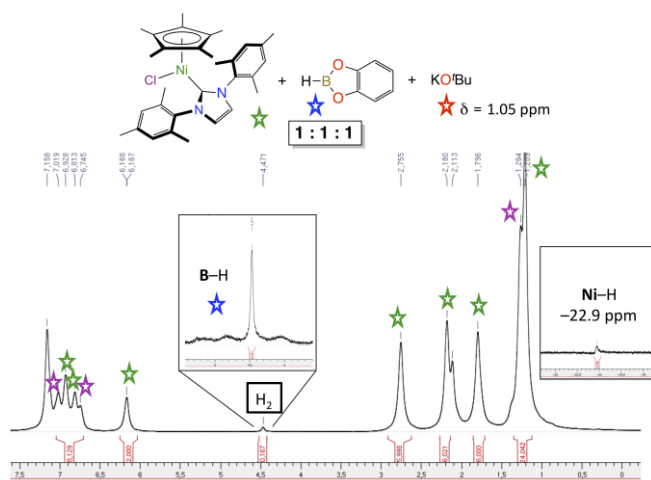


Figure 4. ¹H NMR (C₆D₆, 293 K) spectrum of a **2a** / HBCat / KOt-Bu (1:1:1) mixture.

present in a ratio of ca. 5% when compared to **2a**, is assigned to a nickel-hydride species by analogy with the corresponding signal of [Ni(Cp)H(IMes)].^{18a} Albeit to a low extent, this suggests that a reaction has well occurred at the nickel centre. In addition to these observations, the proton of the starting HBCat is only observed in very minor proportions, and the singlet belonging to the *tert*-butoxide anion has shifted from 1.05 to 1.28 ppm, which corresponds to the shift observed when the latter is reacted with HBCat in the absence of nickel pre-catalyst, and thus suggests that the main reaction occurred between these two species under these conditions.

To gain further insight into this reaction, we next recorded the ¹¹B NMR spectrum of a 1:1 mixture of HBCat and KOt-Bu in C₆D₆ at room temperature (Fig. 5). In agreement with the data reported by the groups of S. P. Thomas²⁸ and T. B. Clark²⁹ for the reaction of HBPIn with NaOt-Bu, several peaks are observed, which can be attributed to BH₃ (or more likely to B₂H₆) at -13.3 ppm, to (*t*-BuO)BCat at 25.8 ppm, and most importantly to an

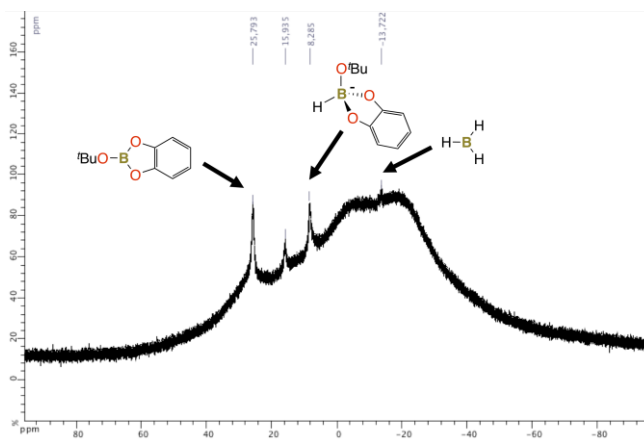
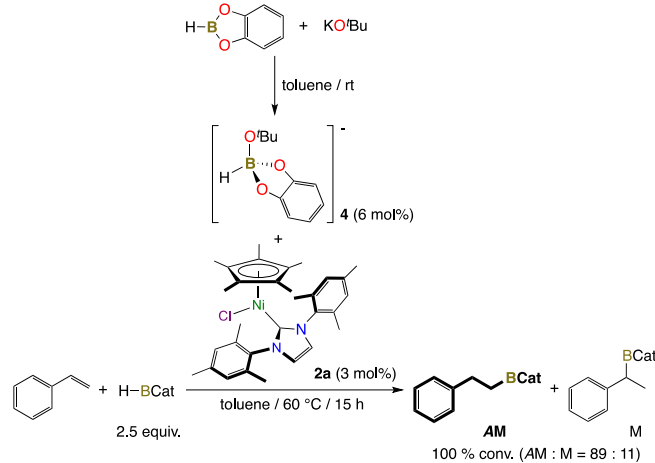


Figure 5. ¹¹B NMR (C₆D₆, 298 K) spectrum of a HBCat / KOt-Bu (1:1) mixture.

alkoxo-catecholato-borohydride species, [H(*t*-BuO)BCat]⁻ (**4**), at 8.2 ppm, that has been described to act as a universal reducing agent for a number of iron, cobalt, nickel and manganese complexes in various hydrofunctionalization reactions.^{12b,28,30}

The addition of this preformed mixture (6 mol%) and HBCat (2.5 equiv.) to **2a** (3 mol%), previously solubilized in toluene in the presence of styrene, resulted in a catalytic system that demonstrated similar activity to when **4** is generated *in situ* (Scheme 3), thus suggesting that this species could also act as the pre-catalyst activator here.

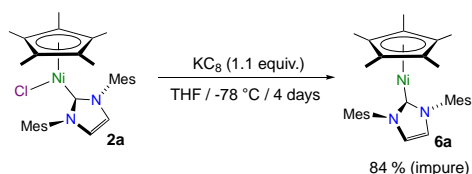


Scheme 3. Addition of preformed **4** to a catalytic reaction mixture.

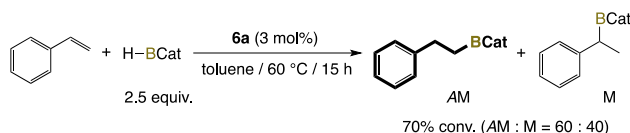
We were intrigued by the observation of a strong effervescence at the beginning of each catalytic reaction, *i.e.*: immediately after the addition of HBCat, and this independently of the presence or absence of styrene (the latter being indifferently added before or after HBCat). So, we next conducted a piezometric study in order to quantify the amount of H₂ produced. For that purpose, we used a thermostatically controlled double-walled Schlenk tube that is connected to a

pressure transducer, which allows the real-time monitoring of the pressure inside the Schlenk (Fig. S1).³¹ Using this experimental set-up, we measured the production of 1 equiv. of H₂ per mole of nickel when 83 equiv. HBCat were added to a 1:2 mixture of **2a** and KO^tBu in toluene at room temperature. Similarly, the reaction of **2a** with 2 equiv. of KO^tBu and 2 equiv. of HBCat produced 1 equiv. of H₂ per mole of nickel. In contrast, the reaction of 1 equiv. **2a** with 1 equiv. KO^tBu and 1 equiv. of HBCat only produced 0.5 equiv. of H₂ per mole of nickel.

In view of these data, we considered the possible implication of the nickel hydride complex [NiCp*H(IMes)] (**5a**), that would act as the true catalytic precursor^{18a} and would be reduced with concomitant H₂ release to the Ni(I) active species, [NiCp*(IMes)] (**6a**), whose IPr analogues (Cp and Cp*) have already been isolated³² and shown to be catalytically competent in Suzuki couplings.³³ To try to validate this possibility, we then prepared **6a** by reacting **2a** with KC₈ (or Na/Hg) in THF at -78 °C (Scheme 4). The generation of **6a** was established by ¹H NMR spectroscopy. Two highly deshielded singlets at 107 and 31 ppm, integrating for 15 and 2 protons respectively (Fig. S2), could indeed be assigned to the protons of the Cp* group and of the imidazolylidene ring by comparison with the reported data for [NiCp*(IPr)].³² However, despite repeated attempts, we have been unable to isolate it pure due to its high sensitivity. Nevertheless, we still attempted the hydroboration of styrene with HBCat in the presence of impure **6a** (3 mol%). 70 % conversion was observed after 15 h at 60 °C, with a 60:40 AM/M ratio (Scheme 5). Despite the reduced performance and selectivity compared to **2a** and KO^tBu, which may be attributed to the presence of impurities, this result, observed in the absence of KO^tBu, tended to confirm the implication of **6a** in the catalytic cycle.



Scheme 4. Synthesis of **6a**.



Scheme 5. Hydroboration of styrene catalysed by **6a**.

From that point on, different mechanisms for the hydroboration of styrene by HBCat catalysed by **6a** were then considered. Density functional theory (DFT) computations at the PBE-D3(BJ)/def2-TZVPP level of theory were carried out to discriminate between the different hypothesis that were formulated. For this study, only reaction intermediates (local

energy minima) were considered, and no transition state (energy saddle-points) were searched for. Thus, only the thermodynamics of the reactions were studied, with no insight into the kinetics. Reaction Gibbs energies computed at this level of theory are compiled in Table 1 at both temperatures considered in the experimental part of this work, *i.e.*: at 25 °C and 60 °C.

Two reactions were considered for the formation of the Ni(I) catalyst **6a** from the Ni(II) hydride **6a**: (i) one where **5a** would react with an equivalent of **4**, which would act as a reductant, to generate **6a** and one equivalent of H₂; (ii) the other where two molecules of **5a** would react together to generate two equivalents of **6a** and one of H₂. In these two reactions, both reactants should lose a hydrogen radical. Both of these reactions have been found to be endergonic with the former being largely less favourable than the latter at both 25 °C ($\Delta_r G^0 = 53.66$ vs. 13.82 kcal/mol) and 60 °C ($\Delta_r G^0 = 52.38$ vs. 13.12 kcal/mol). Examples of reactions similar to the latter have been

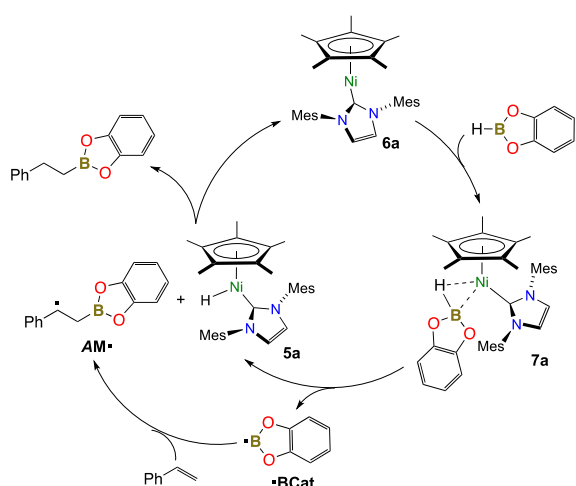
Table 4. Reaction Gibbs energies computed at the PBE-D3(BJ)/def2-TZVPP level of theory

Reaction	$\Delta_r G^0$ at 25 °C (kcal/mol)	$\Delta_r G^0$ at 60 °C (kcal/mol)
5a + HBCatO ^t Bu ⁻ → 6a + BcatO ^t Bu ⁻ + H ₂	53.66	52.38
5a → 6a + ½ H ₂	13.82	13.12
6a + HBCat → 7a	-6.77	-4.94
7a → 5a + Bcat [•]	43.85	42.14
7a + styrene → 8a	17.80	19.74
Bcat [•] + styrene → AM [•]	-41.96	-40.29
Bcat [•] + styrene → M [•]	-26.72	-25.08
8a → 5a + AM [•]	-14.84	-16.79
8a → 5a + M [•]	0.40	-1.58
AM [•] + 5a → 6a + AM	-12.82	-12.95
M [•] + 5a → 6a + M	-24.77	-24.87

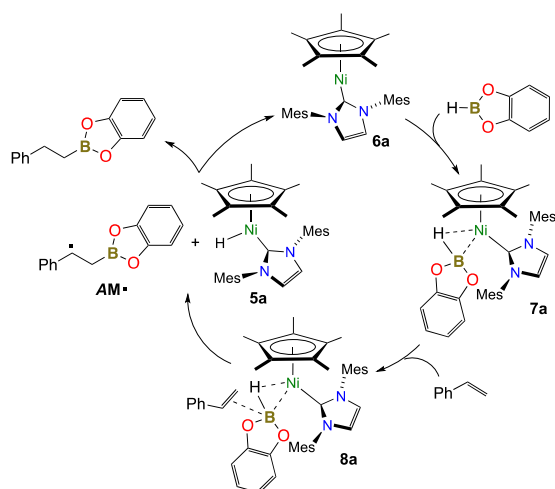
known for more than 40 years,³⁴ and even if this reaction is endergonic, the equilibrium should be shifted toward the formation of **6a** as a consequence of the law of mass action since H₂ mostly escapes the solution as a gas, as observed experimentally.

The first step of the catalytic cycle was initially supposed to be an oxidative addition of **6a** to HBCat to generate a Ni(III) intermediate, as CV measurements suggested a Ni(I)/Ni(III) catalytic cycle could be amenable. However, all DFT attempts to optimize such a structure led instead to the “agostic” adduct **7a** where the H–B bond of the HBCat attractively interacts with the Ni(I) centre in an exergonic fashion at both 25 °C ($\Delta_r G^0 = -6.77$ kcal/mol) and 60 °C ($\Delta_r G^0 = -4.94$ kcal/mol). Mapping the spin density of this adduct revealed an important single electron population on the hydrogen involved in the agostic interaction, giving it a strong hydrogen radical character (Fig. S3).

From this agostic intermediate, two mechanisms have been considered: (i) a first one where the B–H bond would undergo an homolytic fission to generate a boron radical that will then be captured by the styrene forming a carbon radical and **5a** (Scheme 6); or (ii) a second one where an adduct **8a** between **7a** and a styrene (Fig. S4) would homolytically break the B–H bond and release the same carbon radical as in the previous mechanism and **5a** (Scheme 7). In both cases, the carbon radical would then react with **5a** to regenerate **6a** and yield the final hydroboration product. Figure 6 shows the Gibbs energy profiles for both considered mechanisms of the catalytic cycle, leading to both products (**AM** and **M**) at 25 °C and 60 °C. The second step of both these mechanism, the only one by which they differ, is endergonic but the reaction Gibbs energy is more than twofold larger in mechanism 1 than in mechanism 2, at both considered temperatures. The final product **AM** is predicted to be more stable than its regioisomer **M**, in agreement with the experimental results. The difference of stability between **AM** and



Scheme 6. Proposed catalytic mechanism 1 (outer-sphere transfer), through the release of a boron radical.



Scheme 7. Proposed catalytic mechanism 2 (inner-sphere transfer), through the formation of the adduct **8a**.

M does not vary between 25 °C and 60 °C [$\Delta(\Delta_r G^0) = -3.29$ kcal/mol in both cases]. Hence, the experimentally observed difference in regioselectivity with the temperature seems to arise from the third step of the mechanism, *i.e.*: the formation of the carbon radical **AM**[•] or **M**[•]. As expected, **AM**[•] is more stable than **M**[•], the difference in stability being larger than between **AM** and **M**, but this stability difference does not vary much with the temperature [$\Delta(\Delta_r G^0(25\text{ °C})) = -15.24$ kcal/mol vs. $\Delta(\Delta_r G^0(60\text{ °C})) = -15.21$ kcal/mol]. However, considering mechanism 2, this step is exergonic at both temperatures for the formation of **AM**[•], but goes from slightly exergonic at 60 °C to slightly endergonic at 25 °C for the formation of **M**[•].

Considering these data, we propose the following mechanism. The reaction of an equivalent of **4** with **2a** could

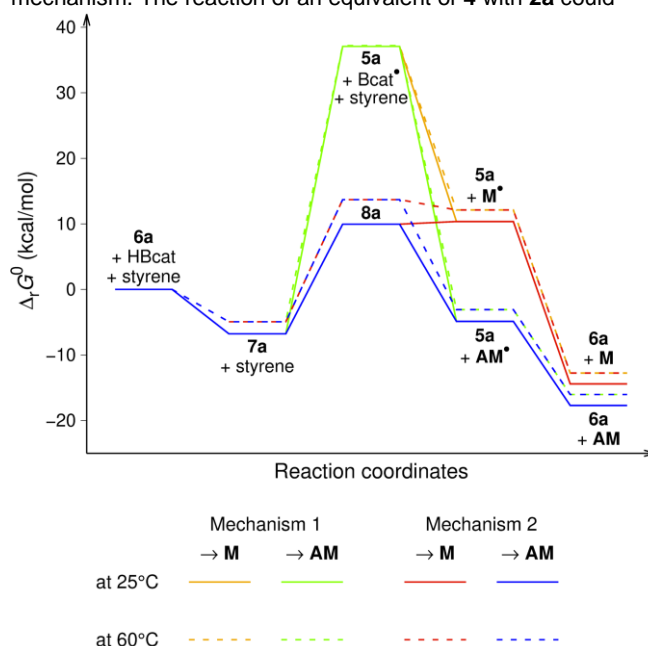
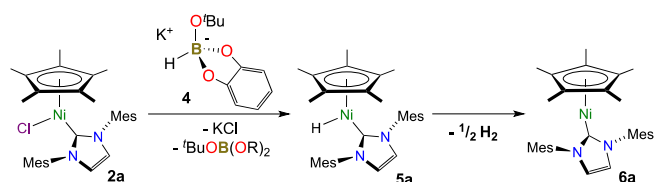


Figure 6. Gibbs energy profiles for the catalytic cycle following mechanism 1 in orange (synthesis of **M**) and green (synthesis of **AM**), or mechanism 2 in red (synthesis of **M**) and blue (synthesis of **AM**) at 25 °C (solid lines) and 60 °C (dashed lines).

generate the corresponding nickel hydride species **5a**, possibly through a σ -bond metathesis mechanism, which contrasts with the commonly proposed formation of a putative nickel alkoxide intermediate that would then react with the borane^{16c} (or silane^{18b35}) to generate the Ni(II) hydride intermediate. Then, in an initiation step, two **5a** could react together to generate the catalytically active Ni(I) species **6a** (Scheme 8).³⁶ The latter would then form an “agostic” intermediate **7a**, where the B–H bond of the borane interacts with the Ni(I). Styrene would then form an adduct **8a** with **7a** before homolytically breaking the B–H bond, hence regenerating **5a** and releasing a carbon radical. This carbon radical would finally react with **5a**, to yield the

hydroboration product and regenerating **6a** (Scheme 7). Importantly, this mechanism is in agreement with our previous observation, in the related hydrosilylation reaction of carbonyl derivatives catalysed by **1a**,^{18a} where we noted that although a Ni(II)–H species is most probably the true catalytic precursor, there is no insertion of the C=O or C=C double bond into this Ni(II)–H bond.



Scheme 8. Proposed mechanism for the generation of the Ni(I) active species **6a**.

Conclusions

In conclusion, we have shown that the [NiCp*Cl(I)Mes] complex **2a** is an efficient precatalyst for the hydroboration of alkenes in the presence of a catalytic amount of KO t -Bu. With HBCat, about ten styrene derivatives and vinylicyclohexane have been converted to the linear product with yields ranging from moderate to very good depending on the substrate. The use of HBPIn instead of HBCat allowed to obtain the branched product as the major one in the cases of styrene, 4-trifluoromethylstyrene and 4-methoxystyrene.

Mechanistic studies strongly suggest the initial generation of a the nickel-hydride complex **5a** by reaction of **2a** with the *in situ* formed *tert*-butoxy-catecholato-borohydride species [H(*t*-BuO)BCat] (**4**), as evidenced by ¹H and ¹¹B NMR spectroscopy. Two molecules of the latter would then react together to generate two equivalents of the Ni(I) species **6a** and one equivalent of H₂, as suggested by combined experimental and theoretical studies. The latter would then act as the active species through a catalytic cycle involving an agostic intermediate **7a** and a styrene adduct **8a** that would homolytically break the B–H bond of the borane. These unprecedented studies with only the fourth nickel hydroboration catalyst reported to date¹⁶ shed light both on the potential of nickel as another base metal for this important transformation, and on the fact that appropriately designed nickel(I) species may be an interesting lead for future research in this domain.

Experimental Section

General comments

All reactions were carried out using a glovebox or standard Schlenk techniques under an atmosphere of dry argon. Solvents were distilled from appropriate drying agents under argon. Unless otherwise specified, solution NMR spectra were recorded at 298 K on Bruker Avance I 300 MHz, or Bruker Avance III HD 400 MHz spectrometers operating at

300.13 or 400.13 MHz for ¹H, at 75.47 or 100.61 MHz for ¹³C and at 96.29 or 128.38 MHz for ¹¹B. The chemical shifts are referenced to the residual deuterated or ¹³C solvent peaks. Chemical shifts (δ) and coupling constants (J) are expressed in ppm and Hz respectively. The catalyst precursors **1a**,³⁷ **1b**,^{17b} **1c**,³⁸ **2a**,³⁹ **2b**,³⁹ and **3a**^{17f} were prepared according to published procedures.

General procedure for the hydroboration of alkenes

In an oven dried Schlenk tube were added **2a** (17 mg, 0.0318 mmol, 3 mol%), KO t -Bu (7 mg, 0.0624 mmol, 6 mol%), and toluene (2 mL), containing the internal standard (trimethoxybenzene, 0.6 mg/mL). This was followed by the addition of HBCat (0.266 mL, 2.50 mmol, 2.5 equiv.) or HBPIn (0.363 mL, 2.50 mmol, 2.5 equiv.) and of the desired alkene (1.00 mmol, 1 equiv.). The resulting reaction mixture was stirred in a preheated oil bath at 60 °C for 15 h. The solution was then cooled to room temperature and an aliquot of the mixture was removed by syringe in order to determine the conversion and the isomeric ratio by ¹H NMR spectroscopy. The rest of the solution was filtered through a plug of silica that was washed with CH₂Cl₂. The resulting filtrate was dried under high vacuum to give a pale orange solid (with HBCat) or a pale yellow oil (with HBPIn). The purification procedure was performed rapidly because of the fast degradation of the desired products, especially with HBCat.²² The branched isomer, in particular, was found to be very unstable upon filtration over the silica plug, allowing the isolation of the pure linear isomer with HBCat and generating (in some cases) an increase of the linear/branched ratio with HBPIn.

Synthesis of [NiCp*(I)Mes] (**6a**)

In a glovebox, a Schlenk tube was charged with a stirring bar and **2a** (300 mg, 0.562 mmol). The Schlenk tube was then laid in a horizontal position in order to introduce sparkling orange shavings of KC₈ (84 mg, 0.621 mmol) without touching the purple powder. In this position, the Schlenk tube was closed and taken out of the glovebox. **2a** was then dissolved in THF without touching KC₈ (10 mL). While putting the Schlenk tube in a vertical position, the system was plunged into a bath at -78 °C. The temperature was allowed to slowly increase to room temperature and the heterogeneous purple medium was stirred for 4 days. After this time, the resulting dark yellow suspension was filtered through a thin pad of Celite under argon and the filtrate was concentrated under vacuum. The resulting brown powder was dissolved in a small amount of pentane and stored at -28 °C overnight. The mother liquor was removed with a syringe to yield **6a** as a shining yellow-brown powder (234 mg, 0.470 mmol, 84 %) that was dried under high vacuum. ¹H NMR (C₆D₆, 400.13 MHz): δ 107.31 (s v.br., 15H, C₅Me₅), 30.95 (s br., 2H, NCH), 5.29 (s br., 4H, *m*-H), 3.57 (s, 6H, *o*-Me), 2.21 (s, 6H, *p*-Me), 1.42 (s, 6H, *o*-Me).

Control experiments

Investigation of the mercury effect: An oven dried Schlenk tube was charged with **2a** (17 mg, 0.0318 mmol, 3 mol%), KO t -Bu (7 mg, 0.0624 mmol, 6 mol%), and toluene (2 mL), containing the internal standard (trimethoxybenzene, 0.6 mg/mL). This was followed by the addition of Hg (1.2 g, 5.98 mmol, 188 equiv.), HBCat (0.266 mL, 2.50 mmol, 2.5 equiv.), and styrene (0.115 mL, 1.00 mmol, 1 equiv.). The resulting reaction mixture was stirred in a preheated oil bath at 60 °C for 15 h. The solution was then cooled to room temperature and an aliquot of the mixture was removed by syringe in order to determine the conversion and the isomeric ratio by ¹H NMR spectroscopy. A conversion of 100 % with a 90:10 AM/M ratio was observed.

Investigation of the radical scavenger effect: An oven dried Schlenk tube was charged with **2a** (17 mg, 0.0318 mmol, 3 mol%), KO^t-Bu (7 mg, 0.0624 mmol, 6 mol%), and toluene (2 mL), containing the internal standard (trimethoxybenzene, 0.6 mg/mL). This was followed by the addition of HBCat (0.266 mL, 2.50 mmol, 2.5 equiv.), styrene (0.115 mL, 1.00 mmol, 1 equiv.) and TEMPO (156 mg, 1.00 mmol, 1 equiv. (at t = 0 or 7 h) or 5 mg, 0.0320 mmol, 3 mol%) or galvinoxyl (422 mg, 1.00 mmol, 1 equiv.). The resulting reaction mixture was stirred in a preheated oil bath at 60 °C for 15 h. The solution was then cooled to room temperature and an aliquot of the mixture was removed by syringe in order to determine the conversion by ¹H NMR spectroscopy. Complete inhibition of the reaction was observed when 1.0 equiv. TEMPO or galvinoxyl was added at t = 0 h. 55% conversion was observed when 3 mol% TEMPO was added at t = 0 h. 76% conversion was observed when 1.0 equiv. TEMPO was added at t = 7h.

¹H NMR follow-up of a 1:1:1 mixture of 2a/HBCat/KOt-Bu: An oven dried Schlenk tube was charged with **2a** (32 mg, 0.0599 mmol), KO^t-Bu (7 mg, 0.0624 mmol) and freeze-pump-thaw degassed C₆D₆ (2 mL). The resulting mixture was cooled -25 °C before the addition of HBCat (6.4 μL, 0.0598 mmol). The reaction mixture was then vigorously stirred for several seconds prior to the transfer of an aliquot of 0.6 mL into an NMR tube placed in a bath at -25 °C. ¹H NMR spectra were then recorded from 253 to 298 K.

¹¹B NMR analysis of a 1:1 mixture of HBCat/KOt-Bu: An oven dried Schlenk tube was charged with KO^t-Bu (42 mg, 0.375 mmol) and freeze-pump-thaw degassed C₆D₆ (2 mL). The resulting mixture was cooled -25 °C before the addition of HBCat (40 μL, 0.375 mmol). The reaction mixture was then vigorously stirred for several seconds prior to the transfer of an aliquot of 0.6 mL into an NMR tube placed in a bath at -25 °C. ¹¹B NMR spectra were then recorded from 253 to 298 K.

Hydroboration of styrene catalysed by 2a with 4: To an oven dried Schlenk tube were added HBCat (0.266 mL, 2.50 mmol, 2.5 equiv.) and KO^t-Bu (7 mg, 0.0624 mmol, 6 mol%) in toluene (2 mL), containing the internal standard (trimethoxybenzene, 0.6 mg/mL) in order to form **4**. This mixture was stirred for 5 min at room temperature before adding **2a** (17 mg, 0.0318 mmol, 3 mol%) and styrene (0.115 mL, 1.00 mmol). The resulting reaction mixture was then stirred in a preheated oil bath at 60 °C for 15 h. The solution was finally cooled to room temperature and an aliquot of the mixture was removed by syringe in order to determine the conversion and the isomeric ratio by ¹H NMR spectroscopy. A conversion of 100 % with a 89:11 AM/M ratio was observed.

Hydroboration of styrene catalysed by 6a: In an oven dried Schlenk tube were added **6a** (15 mg, 0.0301 mmol, 3 mol%) and toluene (2 mL), containing the internal standard (trimethoxybenzene, 0.6 mg/mL). This was followed by the addition of HBCat (0.266 mL, 2.50 mmol, 2.5 equiv.) and styrene (0.115 mL, 1.00 mmol, 1 equiv.). The resulting reaction mixture was stirred in a preheated oil bath at 60 °C for 15 h. The solution was then cooled to room temperature and an aliquot of the mixture was removed by syringe in order to determine the conversion and the isomeric ratio by ¹H NMR spectroscopy. A conversion of 70 % with a 60:40 AM/M ratio was observed.

Cyclic voltammetry

The cyclic voltammogram of complex **3a** (1 mM in CH₃CN) was recorded with a Voltalab 50 potentiostat/galvanostat (Radiometer Analytical MDE150 polarographic stand, PST050 analytical voltammetry and CTV101 speed control unit) controlled by the Voltmaster 4 software. A conventional three-electrode cell (10 cm³) was used in our experiments

with a glassy carbon disk (s = 0.07 cm²) set into a Teflon rotating tube as a working electrode, a Pt wire as a counter electrode, and a KCl (3 M)/Ag/AgCl reference electrode (+210 mV vs. NHE). Prior to each measurement, the surface of the glassy carbon electrode was carefully polished with 0.3 μm aluminum oxide suspension (Escil) on a silicon carbide abrasive sheet of grit 800/2400. Thereafter, the glassy carbon electrode was copiously washed with water and dried with paper towel and argon gas. The electrode was installed into the voltammetry cell along with a platinum wire counter electrode and the reference electrode. The 1 mM solution of **3a** was vigorously stirred and purged with O₂-free (Sigma Oxiclear cartridge) Ar for 15 min before the voltammetry experiment was initiated, and maintained under an Ar atmosphere during the measurement procedure. The voltammogram was recorded at 23(1) °C with 0.1 M NBu₄PF₆ as supporting and inert electrolyte. The voltage sweep rate was set at 200 mV.s⁻¹, and the cyclic voltammogram was recorded from +0.5 V to -2.2 V vs. Fc/Fc⁺.

Piezometric studies³¹

2a, KO^t-Bu and toluene were introduced in a double-walled Schlenk vessel of 28 mL, thermostated at 20 °C under Ar. After the resulting mixture was stirred for a few minutes, a Mykrolis A332984-007 absolute pressure-to-voltage transducer was air-tightly screwed to the neck of the glass vessel and connected to a Pico-Log analog-logic converter/data-logger board interfaced to a computer. This allowed the measurement of the pressure of hydrogen (computed from a linear absolute pressure-output voltage relationship) developed in the known overhead volume of the sealed reactor as a function of time. The absence of leaks was preliminarily checked by applying a moderate pressure of argon gas. HBCat was swiftly injected into the vessel via a lateral glass valve, which was tightly closed immediately upon injection to avoid gas leaks. Several experiments have been performed with varying amounts of reagents: (i) **2a** (48 mg, 0.0899 mmol), KO^t-Bu (20 mg, 0.178 mmol, 2 equiv.) and HBCat (0.799 mL, 7.496 mmol, 83 equiv.) in toluene (6 mL); (ii) **2a** (144 mg, 0.270 mmol), KO^t-Bu (61 mg, 0.544 mmol, 2 equiv.) and HBCat (60 μL, 0.563 mmol, 2 equiv.) in toluene (12 mL); (iii) **2a** (144 mg, 0.270 mmol), KO^t-Bu (30 mg, 0.267 mmol) and HBCat (29 μL, 0.272 mmol) in toluene (12 mL).

Computational details

Geometry optimizations of the different species thought to be involved in the reaction mechanism were performed at the density functional theory (DFT) level of theory, using the ORCA program system⁴⁰ version 4.2.0. The Perdew-Burke-Ernzerhof (PBE) functional⁴¹ augmented with Grimme's D3 dispersion correction with a Becke-Johnson (BJ) damping function⁴² was used for all calculations. All computations were carried out using Karlsruhe's second-generation default triple-ζ valence with two sets of polarization functions (def2-TZVPP) basis set⁴³. Solvent effects were accounted for in all computations by using the conductor-like polarizable continuum model (CPCM),⁴⁴ simulating toluene (ε=2.4, n=1.497) as a solvent. Geometry optimizations by the quasi Newton update procedure with the BFGS update were carried out in all cases with integration grid accuracy 5 to 7, an energy gradient convergence criterion of 10⁻⁴ E_v/a₀, and a tight SCF convergence criterion. All thermodynamic data have been evaluated at 298.15 K and 333.15 K. 3D molecular structures and isosurfaces were produced using Jmol.

Acknowledgements

MJC and VR are grateful to the Université de Strasbourg and the CNRS for their financial help. The Institut Universitaire de

France is acknowledged for its support to VR, and the Région Grand Est for the doctoral fellowship of F. Ulm. Dr. Mourad Elhabiri is gratefully acknowledged for his help with the cyclic voltammetry measurements. YC and JPD thank the Centre de Calcul de l'Université de Strasbourg for providing access to the HPC facilities for the computational part of this work.

Keywords: nickel • hydroboration • alkene • N-heterocyclic carbene • Ni(I) active species

- [1] N. R. Candeias, F. Montalbano, P. M. S. D. Cal, P. M. P. Gois, *Chem. Rev.* **2010**, *110*, 6169-6193.
- [2] J. X. Qiao, P. Y. S. Lam, *Synthesis* **2011**, 829-856.
- [3] G. Berthou-Gelloz, T. Hayashi in *Boronic Acids. Rhodium- and Palladium-Catalyzed Asymmetric Conjugate Addition of Organoboronic Acid*, 2nd Ed. (Ed.: D. G. Hall), Wiley-VCH, Weinheim, **2011**, pp. 263-314.
- [4] A. Suzuki, *Angew. Chem. Int. Ed.* **2011**, *50*, 6722-6737.
- [5] D. G. Hall in *Boronic Acids. Structures, Properties, and Preparation of Boronic Acid Derivatives: Overview of their Reactions and Applications*, 2nd Ed. (Ed.: D. G. Hall), Wiley-VCH, Weinheim, **2011**, pp. 1-134.
- [6] a) T. Ishiyama, M. Murata, N. Miyaoura, *J. Org. Chem.* **1995**, *60*, 7508-7510; b) M. Murata, T. Oyama, S. Watanabe, Y. Masuda, *J. Org. Chem.* **2000**, *65*, 164-168.
- [7] G. C. Fu, *Transition Metal-Catalyzed Hydroboration of Olefins, in Transition Metals for Organic Synthesis: Building Blocks and Fine Chemicals*, 2nd Ed. (Eds.: M. Beller, C. Bolm), Wiley-VCH, Weinheim, **2008**.
- [8] J. V. Obligation, P. J. Chirik, *Nature Rev. Chem.* **2018**, *2*, 15-34.
- [9] a) D. Noh, H. Chea, J. Ju, J. Yun, *Angew. Chem. Int. Ed.* **2009**, *48*, 6062-6064; b) D. Noh, S. K. Yoon, J. Won, J. Y. Lee, J. Yun, *Chem. Asian J.* **2011**, *6*, 1967-1969; c) S. C. Schmid, R. Van Hoveln, J. W. Rigoli, J. M. Schomaker, *Organometallics* **2015**, *34*, 4164-4173; d) H. A. Kerchner, J. Montgomery, *Org. Lett.* **2016**, *18*, 5760-5763.
- [10] a) J. V. Obligation, P. J. Chirik, *J. Am. Chem. Soc.* **2013**, *135*, 19107-19110; b) L. Zhang, Z. Zuo, X. Leng, Z. Huang, *Angew. Chem. Int. Ed.* **2014**, *53*, 2696-2700; c) L. Zhang, Z. Zuo, X. Wan, Z. Huang, *J. Am. Chem. Soc.* **2014**, *136*, 15501-15504; d) W. N. Palmer, T. Diao, I. Pappas, P. J. Chirik, *ACS Catal.* **2015**, *5*, 622-626.
- [11] a) J. Y. Wu, B. Moreau, T. Ritter, *J. Am. Chem. Soc.* **2009**, *131*, 12915-12917; b) J. V. Obligation, P. J. Chirik, *Org. Lett.* **2013**, *15*, 2680-2683; c) L. Zhang, D. Peng, X. Leng, Z. Huang, *Angew. Chem. Int. Ed.* **2013**, *52*, 3676-3680; d) J. Zheng, J.-B. Sortais, C. Darcel, *ChemCatChem* **2014**, *6*, 763-766; e) J. Chen, T. Xi, Z. Lu, *Org. Lett.* **2014**, *16*, 6452-6455.
- [12] a) C. Zhang, H. Zeng, J. Wu, Z. Yin, S. Zheng, J. C. Fettingler, *Angew. Chem. Int. Ed.* **2016**, *55*, 14369-14372; b) J. R. Carney, B. R. Dillon, L. Campbell, S. P. Thomas, *Angew. Chem. Int. Ed.* **2018**, *57*, 10620-10624.
- [13] I. D. Gridnev, N. Miyaoura, A. Suzuki, *Organometallics* **1993**, *12*, 589-592.
- [14] a) S. Crotti, F. Bertolini, F. Macchia, M. Pineschi, *Org. Lett.* **2009**, *11*, 3762; b) R. J. Ely, Z. Yu, J. P. Morken, *Tetrahedron Lett.* **2015**, *56*, 3402.
- [15] a) K. Hirano, H. Yorimitsu, K. Oshima, *Org. Lett.* **2007**, *9*, 5031-5033; b) J.-F. Li, Z.-Z. Wei, Y.-Q. Wang, M. Ye, *Green Chem.* **2017**, *19*, 4498-4502; c) T. Kamei, S. Nishino, T. Shimada, *Tetrahedron Lett.* **2018**, *59*, 2896-2899; d) G. Vijaykumar, M. Bhunia, S. K. Mandal, *Dalton Trans.* **2019**, *48*, 5779-5784.
- [16] a) G. W. Kabalka, C. Narayana, N. K. Reddy, *Synth. Commun.* **1994**, *24*, 1019-1023; b) S. Perreira, M. Srebnik, *Tetrahedron Lett.* **1996**, *37*, 3283-3286; c) E. E. Tourney, R. Van Hoveln, C. T. Buttke, M. D. Friedberg, I. A. Guzei, J. M. Schomaker, *Organometallics* **2016**, *35*, 3436-3439.
- [17] a) T. K. Macklin, V. Snieckus, *Org. Lett.* **2005**, *7*, 2519-2522; b) R. A. Kelly, N. M. Scott, S. Díez-González, E. D. Stevens, S. P. Nolan, *Organometallics* **2005**, *24*, 3442-3447; c) W. Buchowicz, A. Kozioł, L. B. Jerzykiewicz, T. Lis, S. Pasynkiewicz, A. Pęcherzewska, A. Pietrzykowski, *J. Mol. Catal. A* **2006**, *257*, 118-123; d) D. A. Malyshev, N. M. Scott, N. Marion, E. D. Stevens, V. P. Ananikov, I. P. Beletskaya, S. P. Nolan, *Organometallics* **2006**, *25*, 4462-4470; e) W. Buchowicz, W. Wojtczak, A. Pietrzykowski, A. Lupa, L. B. Jerzykiewicz, A. Makal, K. Wozniak, *Eur. J. Inorg. Chem.* **2010**, 648-656; f) V. Ritleng, A. M. Oertel, M. J. Chetcuti, *Dalton Trans.* **2010**, 39, 8153-8160; g) A. M. Oertel, V. Ritleng, L. Burr, M. J. Chetcuti, *Organometallics* **2011**, *30*, 6685-6691; h) A. M. Oertel, V. Ritleng, M. J. Chetcuti, *Organometallics* **2012**, *31*, 2829-2840; i) M. Henrion, M. J. Chetcuti, V. Ritleng, *Chem. Commun.* **2014**, *50*, 4624-4627; j) Y. Wei, A. Petronilho, H. Mueller-Bunz, M. Albrecht, *Organometallics* **2014**, *33*, 5834-5844; k) L. Banach, P. A. Guńka, D. Górska, M. Podlewska, J. Zachara, W. Buchowicz, *Eur. J. Inorg. Chem.* **2015**, 5677-5686; l) F. P. Malan, E. Singleton, P. H. van Rooyen, M. Landman, *J. Organomet. Chem.* **2016**, *813*, 7-14; m) L. Banach, P. A. Guńka; W. Buchowicz, *Dalton Trans.* **2016**, *45*, 8688-8692; n) S. Ando, H. Matsunaga, T. Ishizuka, *J. Org. Chem.* **2017**, *82*, 1266-1272.
- [18] a) L. P. Bheeter, M. Henrion, L. Brelot, C. Darcel, M. J. Chetcuti, J.-B. Sortais, V. Ritleng, *Adv. Synth. Catal.* **2012**, *354*, 2619-2624; b) L. Postigo, B. Royo, *Adv. Synth. Catal.* **2012**, *354*, 2613-2618; c) Y. Wei, S.-X. Liu, H. Mueller-Bunz, M. Albrecht, *ACS Catal.* **2016**, *6*, 8192-8200; d) M. Rocquin, V. Ritleng, S. Barroso, A. M. Martins, M. J. Chetcuti, *J. Organomet. Chem.* **2016**, *808*, 57-62; e) F. Ulm, A. I. Poblador-Bahamonde, S. Choppin, S. Bellemin-Laponnaz, M. J. Chetcuti, T. Achard, V. Ritleng, *Dalton Trans.* **2018**, *47*, 17134-17145.
- [19] L. P. Bheeter, M. Henrion, M. J. Chetcuti, C. Darcel, V. Ritleng, J.-B. Sortais, *Catal. Sci. Technol.* **2013**, *3*, 3111-3116.
- [20] a) S. Z. Tasker, E. A. Standley, T. F. Jamison, *Nature* **2014**, *509*, 299-309; b) M. Henrion, V. Ritleng, M. J. Chetcuti, *ACS Catal.* **2015**, *5*, 1283-1302; c) V. P. Ananikov, *ACS Catal.* **2015**, *5*, 1964-1971; d) V. Ritleng, M. Henrion, M. J. Chetcuti, *ACS Catal.* **2016**, *6*, 890-906.
- [21] A. J. MacNair, C. R. P. Millet, G. S. Nichol, A. Ironmonger, S. P. Thomas, *ACS Catal.* **2016**, *6*, 7217-7221.
- [22] a) K. Burgess, W. A. van der Donk, S. A. Westcott, T. B. Marder, R. T. Baker, J. C. Calabrese, *J. Am. Chem. Soc.* **1992**, *114*, 9350-9359; b) S. A. Westcott, H. P. Blom, T. B. Marder, R. T. Baker, J. C. Calabrese, *Inorg. Chem.* **1993**, *32*, 2175-2182.
- [23] A possible explanation for the observation of a mixture of products with 1-heptene may be due alkene chain isomerization, see reference 10a.
- [24] L. P. Bheeter, D. Wei, V. Dorcet, T. Roisnel, P. Ghosh, J.-B. Sortais, C. Darcel, *Eur. J. Inorg. Chem.* **2015**, 5226-5231.
- [25] J. A. Widegren, R. G. Finke, *J. Mol. Catal. A* **2003**, *198*, 317-341.
- [26] O. R. Luca, B. A. Thompson, M. K. Takase, R. H. Crabtree, *J. Organomet. Chem.* **2013**, *730*, 79-83.
- [27] M. N. Peñas-Defrutos, C. Bartolomé, P. Espinet, *Organometallics* **2018**, *37*, 3533-3542.
- [28] J. H. Docherty, J. Peng, A. P. Dominey, S. P. Thomas, *Nature Chem.* **2017**, *9*, 595-600.
- [29] I. P. Query, P. A. Squier, E. M. Larson, N. A. Isley, T. B. Clark, *J. Org. Chem.* **2011**, *76*, 6452-6456.
- [30] For relevant borohydride species, see: a) H. C. Brown, B. Nazer, J. A. Sikorski, *Organometallics* **1983**, *2*, 634-637; b) H. Wen, L. Zhang, S. Zhu, G. Liu, Z. Huang, *ACS Catal.* **2017**, *7*, 6419-6425.
- [31] a) M. Hamdaoui, M. Ney, V. Sarda, L. Karmazin, C. Bailly, N. Sieffert, S. Dohm, A. Hansen, S. Grimme, J.-P. Djukic, *Organometallics* **2016**, *35*, 2207-2223; b) M. Hamdaoui, C. Desrousseaux, H. Habbita, J.-P. Djukic, *Organometallics* **2017**, *36*, 4863-4884.
- [32] S. Pelties, D. Herrmann, B. de Bruin, F. Hartl, R. Wolf, *Chem. Commun.* **2014**, *50*, 7014-7016.
- [33] J. Wu, A. Nova, D. Balcells, G. W. Brudvig, W. Dai, L. M. Guard, N. Hazari, P.-H. Lin, R. Pokhrel, M. K. Takase, *Chem. Eur. J.* **2014**, *20*, 5327-5337.
- [34] a) J. Evans, J. R. Norton, *J. Am. Chem. Soc.* **1974**, *96*, 7577-7578; b) G. Trinquier, R. Hoffmann, *Organometallics* **1984**, *3*, 370-380; c) J. P. Collman, J. E. Hutchison, P. S. Wagenknecht, N. S. Lewis, M. A. Lopez, R. Guillard, *J. Am. Chem. Soc.* **1990**, *112*, 8206-8208; d) J. P. Collman, P. S. Wagenknecht, N. S. Lewis, *J. Am. Chem. Soc.* **1992**, *114*, 5665-5673; e) B. A. Schaefer, G. W. Margulieux, B. L. Small, P. J. Chirik, *Organometallics* **2015**, *34*, 1307-1320; f) N. X. Gu, P. H. Oyala, J. C. Peters, *J. Am. Chem. Soc.* **2018**, *140*, 6374-6382.
- [35] B. L. Tran, M. Pink, D. J. Mendiola, *Organometallics* **2009**, *28*, 2234-2243.
- [36] The fact that this mechanism accounts for the production of half a equivalent of H₂ for a molecule of **2a** is in agreement with our piezometric measurement in the presence of 1:1:1 mixture of **2a**, KO^tBu and HBCat. Hence, the apparent contradiction with the measurement of one equivalent of H₂ per molecule of **2a** when 2 equiv. of KO^tBu and HBCat or more are used may arise from an unknown side-reaction.
- [37] C. D. Abernethy, A. H. Cowley, R. A. Jones, *J. Organomet. Chem.* **2000**, *596*, 3-5.
- [38] J. Yau, K. E. Hunt, L. McDougall, A. R. Kennedy, D. J. Nelson, *Beilstein J. Org. Chem.* **2015**, *11*, 2171-2178.
- [39] V. Ritleng, C. Barth, E. Brenner, S. Milosevic, M. J. Chetcuti, *Organometallics* **2008**, *27*, 4223-4228.

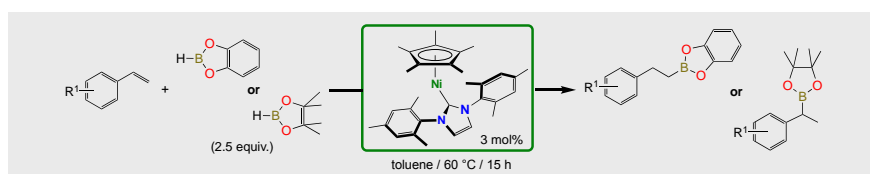
- [40] F. Neese, *WIREs Comput. Mol. Sci.* **2012**, *2*, 73-78.
- [41] J. P. Perdew, K. Burke, M. Ernzerhof, *Phys. Rev. Lett.* **1996**, *77*, 3865-3868.
- [42] a) S. Grimme, J. Anthony, S. Ehrlich, H. Krieg, *J. Chem. Phys.* **2010**, *132*, 154104; b) S. Grimme, S. Ehrlich, L. Goerigk, *J. Comput. Chem.* **2011**, *32*, 1456-1465
- [43] F. Weigend, R. Ahlrichs, *Phys. Chem. Chem. Phys.* **2005**, *7*, 3297-3305.
- [44] V. Barone, M. Cossi, *J. Phys. Chem. A* **1998**, *102*, 1995-2001
-

FULL PAPER

Entry for the Table of Contents (Please choose one layout)

Layout 2:

FULL PAPER



Franck Ulm, Yann Cornaton Jean-Pierre Djukic, Michael J. Chetcuti, Vincent Ritleng**

Page No. – Page No.

Hydroboration of alkenes catalysed by a nickel N-heterocyclic carbene complex: reaction and mechanistic aspects

Initial reduction of the air-stable Ni(II) precursor [NiCp*Cl(IMes)] to the [Ni(I)Cp*(IMes)] active species provides an efficient catalyst for the regioselective hydroboration of alkenes.